Supplement of Adv. Stat. Clim. Meteorol. Oceanogr., 1, 1–14, 2015
http://www.adv-stat-clim-meteorol-oceanogr.net/1/1/2015/
doi:10.5194/ascmo-1-1-2015-supplement

ASCMO
Open Access

Supplement of

Simulation of future climate under changing temporal covariance structures

W. B. Leeds et al.

Correspondence to: W. B. Leeds (william.leeds@climate.com)

S1 Spectral ratio estimation

The following algorithm is used to estimate the ratio of spectral densities for a given smoothness parameter δ. A complete description of the approach is given in Section 2.4. First, set the tolerance level, ϵ_{tol} that indicates when to stop the algorithm. The parameters $\theta_{0,k}$ and $\theta_{1,k}$ represent the logarithm of the spectral density for present and future, respectively, and $I_{0,k}$ and $I_{1,k}$ represent the empirical periodogram at frequency ω_k. Then, initialize $\theta_{0,k}^{(0)}$ and $\theta_{1,k}^{(0)}$ and set $i = 1$. Repeat the following steps until convergence.

1. Set $m_{0,k}^{(i)} = \theta_{0,k}^{(i)} + I_{0,k}\exp(-\theta_{0,k}^{(i)}) - 1$ and $m_{1,k}^{(i)} = \theta_{1,k}^{(i)} + I_{1,k}\exp(-\theta_{1,k}^{(i)}) - 1$.
2. Set $M_{1,k}^{*(i)} = T^{-1/2}\sum_{j=-T/2+1}^{T/2} n_1(m_{1,j} - \theta_{0,j})\exp(-2\pi ijk/T)$.
3. Set $\Lambda_k^{(i)} = (n_1 + \delta k^{2\ell})^{-1} M_{1,k}^{*(i)}$.
4. Set $\lambda_k^{(i)} = T^{-1/2}\sum_{j=-T/2+1}^{T/2} \Lambda_j^{(i)}\exp(2\pi ijk/T)$.
5. Set $\theta_{0,k}^{(i+1)} = (n_1 m_{1,k}^{(i)} + n_0 m_{0,k}^{(i)} - n_1\lambda_k^{(i)})/(n_0 + n_1)$.
6. Set $\theta_{1,k}^{(i+1)} = \lambda_k^{(i)} + \theta_{0,k}^{(i)}$.
7. Stop if $\sum_{k=-T/2+1}^{T/2}\left(\theta_{1,k}^{(i)} - \theta_{1,k}^{(i-1)}\right)^2 < \epsilon_{\text{tol}}$ & $\sum_{k=-T/2+1}^{T/2}\left(\theta_{0,k}^{(i)} - \theta_{0,k}^{(i-1)}\right)^2 < \epsilon_{\text{tol}}$, otherwise set $i = i + 1$ and return to Step 1.

Matlab code to estimate the ratio of two spectral densities is available upon request.

S2 Modulation constant estimation

Here we illustrate how we compute the modulation constants for the deseasonalized observations, $\{\widetilde{Z}_{0,t}\}$. Let $I_t(\omega_k)$ represent an empirical periodogram of $\{\widetilde{Z}_{0,t}, \ldots, \widetilde{Z}_{0,t+44}\}$ for frequency $\omega_k = k/45$. The choice of 45 days windows is in order to accommodate the relatively smooth transition in variability across seasons, but windows of a different length could be chosen. Then, $\overline{I}_t(\omega_k) = \frac{1}{45}\sum_{m=t-44}^{t} I_t(\omega_k)$ is the average of those periodogram estimates, and provides an estimate of the spectral density at frequency ω_k for time t. Now, we also average the estimate across years. For notational convenience, let $\overline{I}_{d,y}(\omega_k)$ represent $\overline{I}_t(\omega_k)$, where d refers to the day of the year ($d = 1, \ldots, 365$ in our case, as our particular

climate model does not have leap years[1]) and y refers to the year ($y = 1, \ldots, n_y$). Then, $\overline{I}_d(\omega_k) = \sum_{y=1}^{n_y} \overline{I}_{d,y}(\omega_k)$, and finally we sum up the variability across all frequencies and take the square root to produce the modulation constant for day d,

$$D_d = \frac{\sqrt{\sum_k \overline{I}_d(\omega_k)}}{\exp\left(\frac{1}{365}\sum_d \log\left(\sqrt{\sum_k \overline{I}_d(\omega_k)}\right)\right)},$$

so that $\sum_d \log(D_d) = 0$.

Figures S1 and S2 show the log-periodograms for the original deseasonalized time series and the deseasonalized and demodulated time series. Matlab code to estimate the demodulation constants is available upon request.

S3 Numerical study

In this section we present results from a numerical study to illustrate the validity of our approach. Define

$$Z_{1,t} = \frac{1}{T^{1/2}} \sum_k e^{-\imath\omega_k t} \sqrt{\rho(\omega_k)} \sum_{s=0}^{T-1} Z_{0,s} e^{\imath\omega_k s}.$$

Then

$$\mathrm{Cov}(Z_{1,t_1}, Z_{1,t_0}) = \frac{1}{T} \sum_{s,s'=0}^{T-1} \gamma_0(s-s') \sum_k e^{\imath\omega_k(s-t_1)} \rho(\omega_k) \sum_l e^{\imath\omega_l(s-t_0)} \rho(\omega_l).$$

We consider the simple case of an AR(1) model:

$$Z_{0,t} = \alpha_{Z_0} Z_{0,t-1} + \epsilon_{Z,t},\ \epsilon_{Z,t} \overset{iid}{\sim} N(0, \sigma^2_{Z_0}),$$

which has the known spectral density

$$f_0(\omega) = \frac{\sigma^2_{Z_0}}{|1 - \alpha_{Z_0} \exp(-2\pi\imath\omega)|^2},$$

[1]Note that when demodulating the observations (which do contain leap years), we first compute $\overline{I}_{d,y}(\omega_k)$ for the length of the time series, then remove the $\overline{I}_{d,y}(\omega_k)$ corresponding to leap days before calculating D_d. Then, after D_d is calculated it is estimated for the corresponding leap days using the average of the day before and after.

and for simplicity, assume $\sigma^2_{Z_0} = 1$. For this example, assume the base and scenario period are from an AR(1) model and $\alpha_{Z_0} = 0.9$ and $\alpha_{Z_1} = 0.99$. Figure S3 shows the theoretical covariance matrices for both values of the autoregressive parameter and Figure S4 shows the theoretical semivariograms (e.g., $(1/2)\mathbb{E}[(Z_t - Z_0)^2]$) when $T = 1500$. We modify the DFT of the baseline period covariance based on the known changes to the spectral density. Let $C_0(h) = \mathbb{E}\left[Z_{0,t+h}Z_{0,t}\right]$ represent the covariance of the baseline period and let $C_1(h) = \mathbb{E}\left[Z_{1,t+h}Z_{1,t}\right]$ represent the covariance function of the scenario period. The matrices $\boldsymbol{C}_0$ and $\boldsymbol{C}_1$ represent the covariance matrices for the base and scenario periods, respectively. Where $\boldsymbol{\Phi}$ represents the DFT matrix and $\boldsymbol{F}_{rat}$ represents the diagonal matrix that has the square root of the spectral ratios at the Fourier frequencies along the diagonal, we compute

$$\boldsymbol{C}_1^* = \boldsymbol{\Phi}^{-1}\boldsymbol{F}_{rat}\boldsymbol{\Phi}\boldsymbol{C}_0\boldsymbol{\Phi}\boldsymbol{F}_{rat}\boldsymbol{\Phi}^{-1}$$

which is the covariance matrix for the simulated process. Figure S3 shows the covariance matrix derived from modifying the DFT of the original covariance matrix. The resulting covariance matrix is nonstationary, with the most significant deviation from the target covariance matrix being near the edges. This is also evident when looking at the semivariogram with origin near the boundary (see Figure S4). When considering the variogram between locations not too near either end of the series, the approximation to the desired variogram is excellent. Thus, for example, Figure S4 shows that $(1/2)\mathbb{E}[(Z_{t+100} - Z_{100})^2]$ under our approach is very close to what it should be for $0 < t < 250$. Thus, at least in this case, we can address inaccuracies in the implied covariance structure by discarding a modest number of observations at the beginning and end of the series.

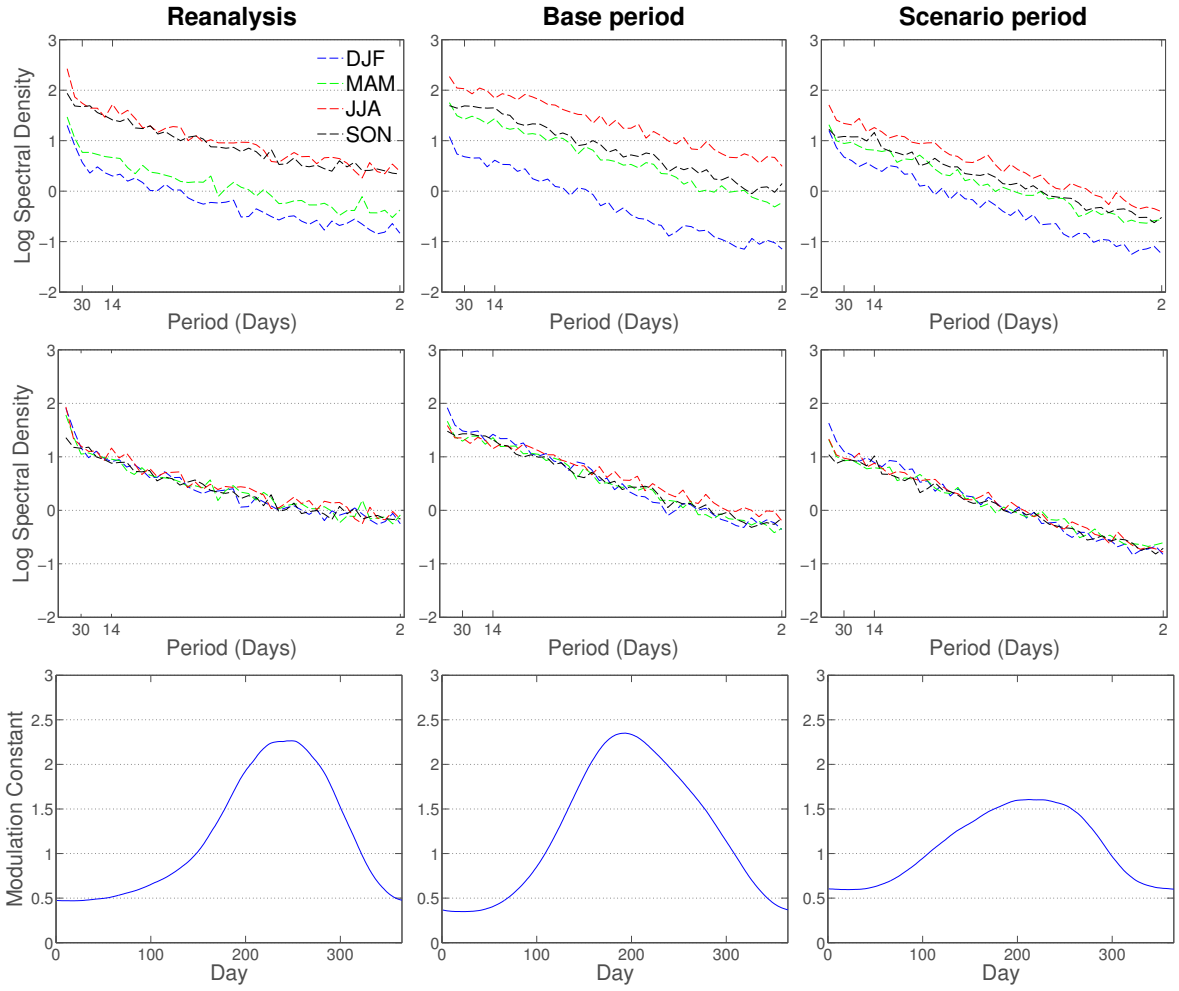

Figure S1: Top: Log of averaged periodograms for the Southern Ocean location, by season, for the reanalysis data (left), base period (middle), and scenario period (right) respectively. Note strongest variability in winter, weakest in summer. The model shows a decrease in the differences in within-season variability across seasons from the base to scenario periods. Middle: identical to top row but now for demodulated time series. Seasonal difference in variability are effectively removed, suggesting we can treat the time series as stationary in time. Bottom: Modulation constants used for the reanalysis data (left), base period (middle) and scenario period (right).

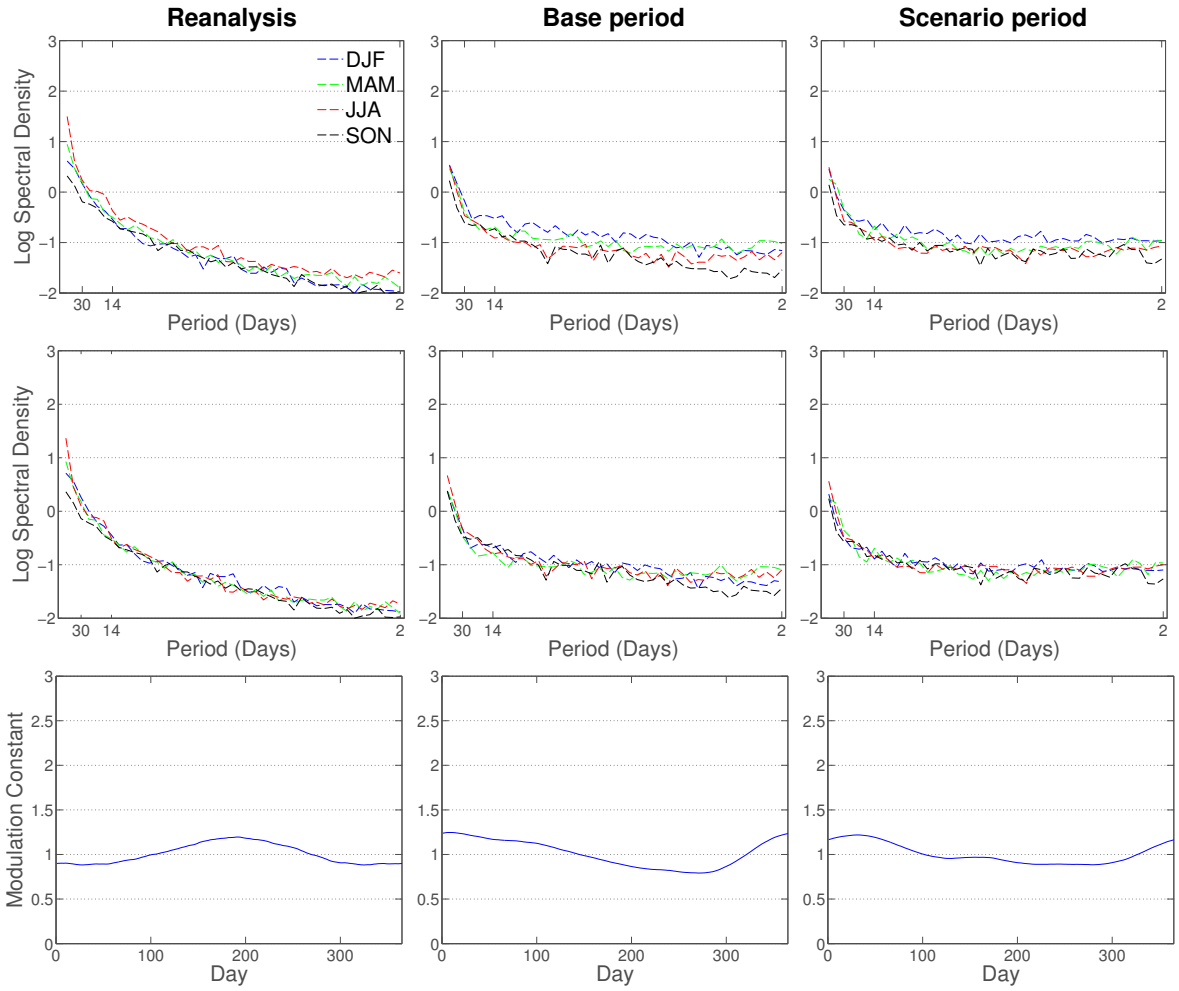

Figure S2: Top: Log of averaged periodograms for the Gulf of Guinea location, by season, for the reanalysis data (left), base period (middle), and scenario period (right) respectively. Middle: Identical to top but now for the demodulated time series. Seasonal differences in variability are effectively removed, suggesting we can treat the time series as stationary in time. Bottom: Modulation constants used for the reanalysis data (left), model baseline period (middle) and model scenario period (right).

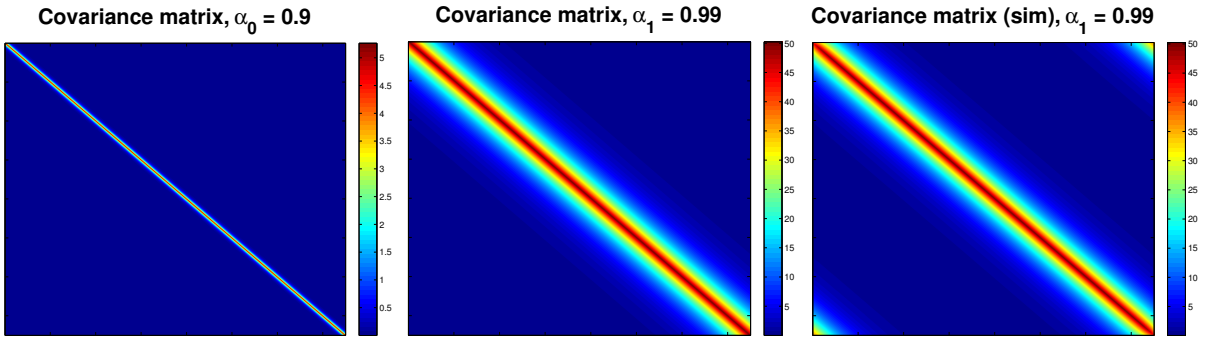

Figure S3: Left: True covariance matrix for an AR(1) process with $\alpha = 0.9$. Middle: True covariance matrix for an AR(1) process with $\alpha = 0.99$. Right: Covariance matrix created by modifying DFT of the process in the left panel. The resulting covariance matrix on the right is nonstationary, with the behavior of the process near the edges exhibiting different characteristics than near the center of the time series.

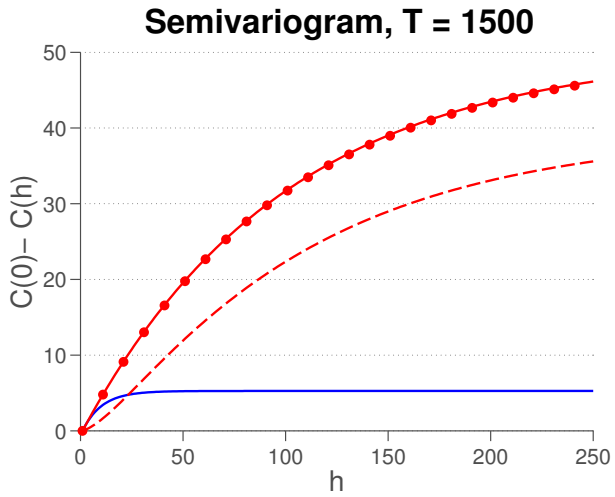

Figure S4: Theoretical semivariogram for the AR(1) process with $\alpha = 0.9$ (solid blue line) and $\alpha = 0.99$ (solid red line), modified semivariogram with origin at Z_0 (red dashed line), and modified semivariogram with origin at Z_{100} (red dotted line), as described in Section S3. The modified semivariogram with origin at Z_{100} tracks the true semivariogram nearly exactly, suggesting that the first and last portions of the simulated time series should be discarded.